Preprint typeset using LaTeX style emulateapj v. 5/2/11

arXiv:1408.3726v2 [astro-ph.GA] 1 Oct 2014

ANTI-HIERARCHICAL EVOLUTION OF THE ACTIVE GALACTIC NUCLEUS SPACE DENSITY IN A HIERARCHICAL UNIVERSE

Motohiro Enoki [1], Tomoaki Ishiyama [2], Masakazu A. R. Kobayashi [3], and Masahiro Nagashima [4, 5]

ABSTRACT

Recent observations show that the space density of luminous active galactic nuclei (AGNs) peaks at higher redshifts than that of faint AGNs. This downsizing trend in the AGN evolution seems to be contradictory to the hierarchical structure formation scenario. In this study, we present the AGN space density evolution predicted by a semi-analytic model of galaxy and AGN formation based on the hierarchical structure formation scenario. We demonstrate that our model can reproduce the downsizing trend of the AGN space density evolution. The reason for the downsizing trend in our model is a combination of the cold gas depletion as a consequence of star formation, the gas cooling suppression in massive halos and the AGN lifetime scaling with the dynamical timescale. We assume that a major merger of galaxies causes a starburst, spheroid formation, and cold gas accretion onto a supermassive black hole (SMBH). We also assume that this cold gas accretion triggers AGN activity. Since the cold gas is mainly depleted by star formation and gas cooling is suppressed in massive dark halos, the amount of cold gas accreted onto SMBHs decreases with cosmic time. Moreover, AGN lifetime increases with cosmic time. Thus, at low redshifts, major mergers do not always lead to luminous AGNs. Because the luminosity of AGNs is correlated with the mass of accreted gas onto SMBHs, the space density of luminous AGNs decreases more quickly than that of faint AGNs. We conclude that the anti-hierarchical evolution of the AGN space density is not contradictory to the hierarchical structure formation scenario.

Subject headings: galaxies: active – galaxies: evolution – galaxies: formation – galaxies: nuclei – quasars: general

1. INTRODUCTION

The space density evolution of active galactic nuclei (AGNs) provides important clues for understanding of physical processes of AGNs and supermassive black hole (SMBH) evolution. In the present day universe, massive and spheroidal galaxies are generally accepted to host SMBHs in the mass range of $10^6 - 10^9\ M_\odot$ in their centers. The masses of SMBHs are observationally found to correlate with physical properties of the spheroidal component of the host galaxies such as stellar mass and velocity dispersion (e.g., Magorrian et al. 1998; Ferrarese & Merritt 2000; Gebhardt et al. 2000; Marconi & Hunt 2003; Häring & Rix 2004; Gültekin et al. 2009; Graham 2012; McConnell & Ma 2013; Kormendy & Ho 2013). These relations suggest that the evolution of SMBHs and AGNs is physically linked to the evolution of galaxies that harbor them. Therefore, in order to study the AGN space density evolution, it is necessary to construct a model that includes prescriptions both for galaxy formation and SMBH/AGN formation.

The current standard galaxy formation paradigm is the hierarchical structure formation scenario in a cold dark matter (CDM) universe. In this scenario, dark halos cluster gravitationally and merge together. In each of dark halos, a galaxy is formed at first. When dark halos merge, the newly formed dark halo contains several galaxies. These galaxies residing in the same host dark halo can merge together due to dynamical friction or random collision. Therefore, more massive galaxies preferentially form at lower redshifts. Thus, massive SMBHs preferentially form at late times as the mass of SMBHs is correlated with the spheroidal stellar component of their host galaxies. If the AGN luminosity were directly correlated with the SMBH mass, bright AGNs would be expected to appear mostly at low redshifts. However, recent optical observations show that the space densities of faint AGNs peak at lower redshifts than those of bright AGNs (e.g., Croom et al. 2009; Ikeda et al. 2011, 2012). This behavior is called *downsizing* or *anti-hierarchical* evolution of AGNs. X-ray observations of AGNs also show the downsizing trend (e.g., Ueda et al. 2003; Hasinger et al. 2005). This anti-hierarchical evolution of the AGN density seems to conflict with the hierarchical structure formation scenario.

In order to explore the evolution of SMBHs/AGNs, many semi-analytic (SA) models of galaxy and AGN formation based on the hierarchical structure formation scenario have been proposed (e.g., Kauffmann & Haehnelt 2000, 2002; Enoki et al. 2003, 2004; Cattaneo et al. 2005; Bower et al. 2006; Croton et al. 2006; Fontanot et al. 2006; Monaco et al. 2007; Somerville et al. 2008). Several recent SA models managed to reproduce the downsizing evolution of AGNs (e.g., Marulli et al. 2008; Bonoli et al. 2009; Fanidakis et al. 2012; Hirschmann et al. 2012; Menci et al. 2013). All of them have changed their models to reproduce the downsizing trend of AGN evolution.

[1] Faculty of Business Administration, Tokyo Keizai University, Kokubunji, Tokyo, 185-8502, Japan; enokimt@tku.ac.jp
[2] Center for Computational Sciences, University of Tsukuba, Tsukuba, Ibaraki, 305-8577, Japan
[3] Research Center for Space and Cosmic Evolution, Ehime University, Matsuyama, Ehime, 790-8577, Japan
[4] Faculty of Education, Nagasaki University, Nagasaki, Nagasaki 852-8521, Japan
[5] Faculty of Education, Bunkyo University, Koshigaya, Saitama, 343-8511, Japan

For example, Hirschmann et al. (2012) modified the SA model of Somerville et al. (2008) by considering several physical recipes for SMBH growth. Menci et al. (2013) used a SA model of galaxy and AGN formation in a warm dark matter (WDM) cosmology instead of the standard ΛCDM cosmology. Some recent cosmological hydrodynamic simulations of galaxy and AGN evolution can also reproduce the downsizing trend of AGN evolution (e.g., Degraf et al. 2010; Hirschmann et al. 2014; Khandai et al. 2014). Although cosmological hydrodynamic simulations can treat the dynamics of gas components, the mass resolution is still insufficient to capture the physical origin of the processes on small scales such as, e.g., star formation, supernova feedback and gas accretion onto SMBHs. These simulations nevertheless seem to be able to capture the essence of how SMBHs grow in reality.

Recent observations of galaxies also show the downsizing behavior of galaxy evolution (see the overview of observations of Fontanot et al. 2009, and references therein). Many SA models and cosmological hydrodynamic simulations also do not correctly reproduce the downsizing trends of galaxy evolution. In particular, SA models and simulations tend to predict the larger space density of low-mass galaxies than observed density at any redshifts. This is because low-mass galaxies are formed too early in SA models and simulations. The overestimation of the space density of low-mass galaxies is a major challenge to most of current SA models and cosmological hydrodynamic simulations (e.g., Fontanot et al. 2009; Cirasuolo et al. 2010; Bower et al. 2012; Weinmann et al. 2012; Guo et al. 2013). However, Henriques et al. (2013) managed to reproduce the observed space density evolution of low-mass galaxies due to a combination of stronger supernova feedback and delayed re-accretion of gas ejected from galaxies by supernova feedback.

In this paper, we focus on investigating whether or not the observed anti-hierarchical trend of the space density evolution of AGNs is contradictory to the hierarchical structure formation scenario. To this end, we use a SA model of galaxy and SMBH/AGN formation. Our SA model is the updated *Numerical Galaxy Catalog* (νGC; Nagashima et al. 2005). νGC is a SA model based on the Mitaka SA model (Nagashima & Yoshii 2004) combined with a cosmological N-body simulation. In this study, we extend νGC to incorporate a SMBH/AGN formation model of Enoki et al. (2003, 2004) and use a new N-body simulation with large box size of Ishiyama et al. (2009, 2012) based on the *WMAP7* cosmology (Komatsu et al. 2011). In contrast to other recent SA models, we adopted a simpler phenomenological SMBH/AGN formation model, which is a purely major merger-driven AGN model, and do not modify our existing SA model, νGC, to reproduce the downsizing trend.

This paper is organized as follows. In Section 2, we briefly describe our SA model, and in Section 3, we present the result of the AGN space density evolution. Finally, in Section 4, we discuss the result of our model.

2. SA MODEL

In SA models, merging histories of dark halos are realized using a Monte Carlo method or cosmological N-body simulations. On top of the formation of dark halos, the evolution of baryonic components is calculated using simple analytic models for gas cooling, star formation, supernova feedback, galaxy merging, and other processes. In this section, we briefly review our SA model, the νGC. Detailed model descriptions are given in Nagashima et al. (2005) for galaxies, and Enoki et al. (2003, 2004) for SMBH/AGN formation.

2.1. *Galaxy Formation Model*

In our SA model, the merging histories of dark halos are directly taken from a new large cosmological N-body simulation. It contains 2048^3 particles within a co-moving box size of 280 h^{-1} Mpc. The gravitational softening length is 4.27 h^{-1} kpc. The particle mass is 1.93×10^8 h^{-1} $M_\odot$. We used the friends-of-friends algorithm (Davis et al. 1985) with a linking length parameter of $b = 0.2$ to identify dark halos. The minimum number of particles identifying a dark halo is 40 and hence the minimum mass of dark halo is 7.72×10^9 h^{-1} $M_\odot$. For the time integration, we used the GreeM code (Ishiyama et al. 2009, 2012), which is a massively parallel TreePM code. The cosmological parameters adopted are based on the concordance ΛCDM cosmological model (*WMAP7*; Komatsu et al. 2011), that is, $\Omega_0 = 0.2725$, $\lambda_0 = 0.7275$, $h = 0.702$, $\Omega_{\rm b} = 0.0455$, $\sigma_8 = 0.807$, and $n_{\rm s} = 0.961$.

When a dark halo is formed, the gas in the halo is shock-heated to the virial temperature of the halo. We refer to this heated gas as the *hot gas* and provide its radial distribution from the halo center as isothermal. The hot gas in central dense regions of the halo simultaneously cools due to efficient radiative cooling. It sinks to the center of the halo and settles into a rotationally supported disk until the subsequent merger of the dark halo. We refer to this cooled gas as the *cold gas*, from which stars can form. The cold gas and stars constitute *galaxies*. In order to avoid the formation of unphysically large galaxies, the gas cooling process is applied only to dark halos with circular velocity $V_{\rm circ} \leq V_{\rm cut}$. In this study, we set $V_{\rm cut} = 260$ km s^{-1}. The halo mass for cooling suppression is $M_{\rm halo} > 5.77 \times 10^{12} \left(V_{\rm cut}/260 \text{ km s}^{-1}\right)^3 \left[\Delta_{\rm vir}(z)/200\right]^{-1/2} M_\odot$; $\Delta_{\rm vir}(z)$ is the ratio of the dark halo density at redshift z to the present critical density. This cooling suppression is similar to the *halo quenching* (Dekel & Birnboim 2006; Cattaneo et al. 2008).

For the star formation rate (SFR) of a galaxy, we adopt the following form

$$\psi(t) = \frac{M_{\rm cold}}{\tau_*}, \tag{1}$$

where $M_{\rm cold}$ is the mass of the cold gas. τ_* is the timescale of star formation, which is determined by

$$\tau_* = \tau_*^0 \left[1 + \left(\frac{V_{\rm d}}{V_{\rm hot}}\right)^{\alpha_*}\right], \tag{2}$$

where $V_{\rm d}$ is the disk rotation velocity. The two free parameters, τ_*^0 and α_*, are chosen to match the observed mass fraction of cold gas in the neutral form in the disks of spiral galaxies. In this study, we adopted $\tau_*^0 = 1.0$ Gyr and $\alpha_* = -5.0$. $V_{\rm hot}$ is a free parameter related to supernova feedback described below. When star formation

takes place, as a consequence, supernovae explosions happen and heat up the surrounding cold gas to the hot gas (*supernova feedback*). The reheating rate of cold gas is given by $\dot{M}_{\rm hot} = \beta_{\rm d}\psi(t)$, where $\beta_{\rm d}$ is the efficiency of reheating due to supernova feedback in disk. We assume that $\beta_{\rm d}$ depends on $V_{\rm d}$, as follows:

$$\beta_{\rm d} = \left(\frac{V_{\rm d}}{V_{\rm hot}}\right)^{-\alpha_{\rm hot}}. \quad (3)$$

The free parameters of $V_{\rm hot}$ and $\alpha_{\rm hot}$ are determined by matching the observed local luminosity function of galaxies. In this study, we adopted $V_{\rm hot} = 100$ km s^{-1} and $\alpha_{\rm hot} = 4$.

When several dark halos have merged, a newly formed larger dark halo contains at least two or more galaxies that had originally resided in the individual progenitor halos. We identify the central galaxy in the newly formed halo with the central galaxy contained in the most massive progenitor halo. Other galaxies are regarded as *satellite galaxies*. These satellites can merge by either dynamical friction or random collisions. Satellite galaxies merge with the central galaxy in the dynamical friction timescale given by Binney & Tremaine (1987). Satellite galaxies sometimes merge with other satellites in the timescale of random collisions. Under the condition that the satellite galaxies are gravitationally bound with each other and merge during encounters, this timescale is given by Makino & Hut (1997). Consider the case that two galaxies of masses m_1 and m_2 ($> m_1$) merge together. If the mass ratio, $f = m_1/m_2$, is larger than a certain critical value of $f_{\rm bulge}$, we assume that a starburst occurs. The entire cold gas content in the progenitor galaxies either turns into bulge stars, is heated up by supernova feedback, or is accreted onto the SMBH. All of the stars pre-existing in merging progenitors and newly formed via starburst are assumed to populate the bulge of a new galaxy. We call such an event a *major merger*. On the other hand, if $f < f_{\rm bulge}$, no starburst occurs and a smaller galaxy is simply absorbed into the bulge of a larger galaxy. Such an event is called a *minor merger*. In this paper, we adopt $f_{\rm bulge} = 0.4$.

Predictions from νGC are in good agreement with many observations of, e.g., luminosity functions of local galaxies, cold gas mass-to-stellar luminosity ratio of spiral galaxies, H I mass functions, galaxy sizes, faint galaxy number counts, redshift distributions for galaxies and the cosmic star formation histories from $z = 0$ to $z = 5$ (Nagashima et al. 2005). However νGC does not correctly reproduce the downsizing evolution of the space density of galaxy. νGC over-predicted the space density of low-mass galaxies. As described in Section 1, many other SA models and cosmological hydrodynamic simulations also do not correctly reproduce the downsizing trends of galaxy evolution. Therefore, this is a common problem in galaxy formation models and simulations based on the hierarchical structure formation scenario, suggesting a lack of our understanding on the interplay between star formation, supernova feedback, gas recycling, and so on. In this paper, we focus only on the downsizing evolution of the AGN space density.

2.2. *SMBH/AGN Formation Model*

In our model, the SMBH mass growth is assumed to be triggered only by merger events. We adopt two processes of SMBH mass growth: (1) SMBH coalescence and (2) accretion of cold gas during major merger of galaxies. We define a SMBH which is powered during a major merger of galaxies as an AGN.

First, we consider the processes of SMBH mass growth. We assume that SMBHs grow through the coalescence of pre-exiting SMBHs when their host galaxies merge. Some hydrodynamic simulations have shown that a major merger of galaxies can drive substantial gaseous inflows and fuels a nuclear starburst leading to the formation of a bulge (e.g., Mihos & Hernquist 1994, 1996; Barnes & Hernquist 1996; Di Matteo et al. 2005; Hopkins et al. 2005, 2006). Thus, we also assume that during a major merger, a fraction of the cold gas, which is proportional to the total mass of stars newly formed at the starburst, is accreted onto the SMBH. All of the cold gas in the progenitor galaxies is depleted by star formation, supernova feedback, or accretion on the SMBH. Under this assumption, the mass of cold gas accreted on the SMBH is given by

$$M_{\rm acc} = f_{\rm BH}\Delta M_{*,\rm burst}, \quad (4)$$

where $f_{\rm BH}$ is a constant and $\Delta M_{*,\rm burst}$ is the total mass of stars formed during the starburst. We set $f_{\rm BH} = 0.0067$ to match the observed relation between masses of host bulges and SMBHs at $z = 0$ found by Häring & Rix (2004) and McConnell & Ma (2013). Figure 1(a) shows the bulge–SMBH mass relations of our SA model and observations. The analytic description for gas, star and SMBH evolution during a starburst event including $\Delta M_{*,\rm burst}$ is described in the Appendix. When a galaxy experiences a major merger for the first time, we assume that the seed SMBH is formed with mass, $M_{\rm acc}$, which is given by Equation (4). As shown in Figure 1(b), the presentday BH mass function predicted by our SA model, is consistent with the observational results of Salucci et al. (1999) and Shankar et al. (2004) although there seems to be an excess of $10^9 M_\odot$ black holes. Our galaxy formation model includes the dynamical friction and the random collision as galaxy merging mechanisms. The mass function for low-mass black holes is determined by the random collision between satellite galaxies. The mass function for high-mass black holes is influenced by the dynamical friction. The bump at $\sim 10^9 M_\odot$ of the mass function originates from the dynamical friction (Enoki et al. 2004).

Next, we consider the light curve of AGNs. The accretion of cold gas during a starburst leads to AGN activity. Following Kauffmann & Haehnelt (2000, 2002), we assume that a fixed fraction of the rest mass energy of the accreted gas is radiated in the B band, and we adopt the B band luminosity of an AGN at time t after a major merger as follows:

$$L_B(t) = \frac{\epsilon_B M_{\rm acc} c^2}{t_{\rm life}} \exp(-t/t_{\rm life}), \quad (5)$$

where ϵ_B is the radiative efficiency in the B-band, $t_{\rm life}$ is the AGN lifetime and c is the speed of light. In our model, we allow for super-Eddington accretion. We assume that $t_{\rm life}$ scales with the dynamical timescale, $t_{\rm dyn}$, as expected if the radius of the ac-

cretion disk were to scale with the radius of the host galaxy (Kauffmann & Haehnelt 2000). The AGN lifetime, $t_{\rm life}$, depends on the redshift of the major merger, since $t_{\rm life} \propto t_{\rm dyn} \propto \rho_{\rm gal}^{-1/2} \propto \Delta_{\rm vir}^{-1/2}(z)$; $\Delta_{\rm vir}(z)$ is the ratio of the dark halo density at the redshift of the major merger to the present critical density. In order to determine the parameter ϵ_B and the present AGN lifetime, $t_{\rm life}(z=0)$, we chose them to match the estimated luminosity function in our model with the observed B-band luminosity function of AGNs at $z=2$. We obtain $\epsilon_B = 0.0055$ and $t_{\rm life}(z=0) = 5.0 \times 10^7$ yr.

Some recent SA models include prescriptions for the *radio-mode AGN feedback*. The radio-mode AGN feedback is due to the radio jet which is powered by hot gas accretion and injects energy into hot gas. Since the radio-mode AGN feedback is a mechanism to quench cooling of hot gas and prevent star formation in massive dark halos, the radio-mode AGN feedback is expected to explain part of the downsizing evolution of galaxies (e.g., Croton et al. 2006; Bower et al. 2006). However, the detailed physics of hot gas heating is still unknown. Moreover, the radio-mode AGN feedback helps to reproduce the observed density of massive galaxies but has hardly any effects on the space density of low-mass galaxies, which are affected by supernova feedback. Our model does not implement the radio-mode AGN feedback. Instead we take a simple approach to suppress gas cooling as described in Section 2.1. The gas cooling process is applied only to halos with circular velocity $V_{\rm circ} \leq V_{\rm cut}$.

3. EVOLUTION OF AGN SPACE DENSITY

In Figure 2, we present the redshift evolution of AGN space density. Solid lines are results of our SA model and symbols with error bars linearly connected with dashed lines are results of observations (Croom et al. 2009; Fontanot et al. 2007; Ikeda et al. 2011, 2012). In order to compare the model result with observations, we convert the absolute B-band magnitude (M_B) into the absolute AB magnitude at 1450 Å (M_{1450}) using the empirical relation given by Shen & Kelly (2012). Our SA model can qualitatively reproduce the downsizing trend of the AGNs space density evolution. While our model overproduces the space density of faint AGN (i.e. $M_{1450} > -24$) at $z \lesssim 1$, it is consistent with the results of GOODS (Fontanot et al. 2007) and COSMOS (Ikeda et al. 2011, 2012) at $z \gtrsim 3$.

In the following, we will discuss the physical reasons responsible for the AGN downsizing trend predicted by our SA model. In our model, SMBHs assemble their mass through cold gas accretion during a major merger and through the coalescence of the two SMBHs themselves. At high redshifts, since galaxies generally contain a larger amount of cold gas, a large amount of the cold gas fuel is provided for being accreted onto a SMBH. The cold gas in a galaxy is depleted over time by star formation. Moreover, the hot gas cooling process is suppressed in massive dark halos. Therefore, the amount of the cold gas accreted onto SMBH decreases with cosmic time. Figure 3 shows the redshift evolution of the logarithmic mean of the ratio of cold gas mass ($M_{\rm cold}$) to stellar mass ($M_{\rm star}$) for galaxies with $M_B < -18$. This shows that the mass fraction of cold gas mass in a galaxy decreases with time and that massive galaxies with massive black holes have a smaller cold gas fraction than less massive galaxies with less massive black holes. Therefore, at low redshifts, a major merger does not necessarily trigger a luminous AGN because the luminosity of AGNs is proportional to the cold gas mass of accreted onto SMBHs. As a result, the space density of luminous AGNs decreases quickly. In addition, Enoki et al. (2004) showed that at $z \lesssim 1$, a dominant process for the mass growth of SMBHs is due to black hole coalescence and not due to gas accretion, since the cold gas decreases with time.

As described in Section 2.2, we allow for super-Eddington accretion. Although we do not calculate bolometric luminosity $L_{\rm bol}$, observational studies have indicated that $L_{\rm bol}$ is smaller than $10L_B$. Therefore, adopting $L_{\rm bol} = 10L_B$, we can obtain the upper limit of the number fraction of super-Eddington AGN ($L_{\rm bol}/L_{\rm Edd} > 1$) from the B-band Eddington ratio ($L_B/L_{\rm Edd}$), which can be calculated in our model. As shown in Figure 4(a), the 90th percentiles of $L_B/L_{\rm Edd}$ is less than unity at $z < 1$ and larger than unity at $1 < z < 4$, which results in the fraction of the super-Eddington AGN of less than 10% at $z < 1$ and $10 \sim 15$% at $1 < z < 4$. The maximum values of $L_B/L_{\rm Edd}$ also indicate that the maximum Eddington ratio is less than 10 at $z < 1$ and $10 \sim 80$ at $1 < z < 4$. The median of the Eddington-ratios of AGNs and the fraction of high Eddington ratio AGNs ($\log[L_B/L_{\rm Edd}] > -1$) decrease with cosmic time. These results are consistent with the observational results of Shen & Kelly (2012) and Nobuta et al. (2012). These trends indicate that the ratio of $\dot{M}_{\rm BH}$ to $M_{\rm BH}$ decreases with time. This suggests that the fraction of AGNs having massive black holes in galaxies that have small cold gas mass becomes larger at lower redshifts.

Figure 4(b) shows the redshift evolution of the mean of the logarithm of the B-band Eddington ratios ($\langle \log[L_B/L_{\rm Edd}] \rangle$) in different magnitude intervals. We find the following from this figure. (1) The Eddington ratio of luminous AGNs is higher than that of faint ones, (2) the Eddington ratio of luminous AGNs is almost constant against redshift, and (3) the Eddington ratio of faint AGNs decreases with cosmic time. In our model, the luminosity of AGNs is determined by Equation (5), in which it depends on the cold gas mass, not on the SMBH mass. Thus only AGNs that have large amount of cold gas can be luminous. The amount of cold gas generally decreases with cosmic time, while the SMBH mass increases with cosmic time. Therefore, the Eddington ratio of faint AGNs decreases with cosmic time.

In our model, we assume that the AGN lifetime scales with the dynamical timescale of the host galaxy ($t_{\rm life} \propto t_{\rm dyn}$). Since $t_{\rm dyn}$ is shorter at higher redshifts, this assumption is one of the reasons for the AGN downsizing trend. In order to examine this effect, we plot the redshift evolution of AGN space density adopting the constant AGN lifetime model for $t_{\rm life} = 5.0 \times 10^7$ yr in Figure 5 (a). The evolution of AGN space density shows neither anti-hierarchical trend nor hierarchical trend. Thus, the assumption of $t_{\rm life}(z) \propto t_{\rm dyn}$ is not the unique cause of the downsizing evolution of AGNs.

In many previous studies, the radio-mode AGN feedback is expected to provide one important process for predicting the downsizing trend in the space density evo-

lution of galaxies, as it is supposed to solve the so called *over-cooling* problem and thus to regulate the late growth of massive galaxies. In our model, the gas cooling process is suppressed in dark halos with circular velocity $V_{\rm circ} > V_{\rm cut}$. This cooling suppression is similar to the radio-mode AGN feedback. In order to examine this effect of the gas cooling suppression on the evolution of AGN space density, we show the evolution of AGN space density of the model for $V_{\rm cut} = 2000$ km s^{-1} in Figure 5(b). In this *test* model, the gas cooling process is applied to all halos and this corresponds to no radio-mode AGN feedback. Figure 5(b) demonstrates that the AGN space density does not show a hierarchical trend. Therefore, the cause of the downsizing evolution of AGNs is not only the radio-mode AGN feedback, although the radio-mode AGN feedback is an important ingredient for a galaxy formation model.

In summary, the reason for a downsizing trend of AGN evolution in our SA model is a combination of the cold gas depletion as a consequence of star formation, the AGN lifetime scaling with the dynamical timescale, and the gas cooling suppression in massive halos.

4. CONCLUSION AND DISCUSSION

In this study, we have demonstrated that our semi-analytic model of galaxy and SMBH/AGN formation based on the hierarchical structure formation scenario predicts a downsizing trend in the AGN space density evolution in qualitative agreement with observations. Therefore, the observed anti-hierarchical evolution of the AGN space density is not necessarily contradictory to currently favored hierarchical structure formation scenarios. Since the cold gas is mainly depleted by star formation and gas cooling is suppressed in massive dark halos, the amount of cold gas accreted onto SMBHs decreases with cosmic time. Because the luminosity of AGNs is correlated with the mass of accreted gas onto SMBHs, the space densities of bright AGNs decrease more quickly than those of faint AGNs.

Many SA models of galaxy and SMBH/AGN formation have been proposed (e.g., Kauffmann & Haehnelt 2000, 2002; Enoki et al. 2003, 2004; Cattaneo et al. 2005; Bower et al. 2006; Croton et al. 2006; Fontanot et al. 2006; Monaco et al. 2007; Somerville et al. 2008). Several recent SA models managed to reproduce the downsizing evolution of AGNs (e.g., Marulli et al. 2008; Bonoli et al. 2009; Fanidakis et al. 2012; Hirschmann et al. 2012; Menci et al. 2013). Unlike these recent SA models, we adopt a simpler phenomenological SMBH/AGN formation model of Enoki et al. (2003, 2004), which is a purely major merger-driven AGN model. In our model the anti-hierarchical AGN space density evolution is a natural result of a combination of different key mechanisms as discussed in Section 3. We note that we do not modify our existing model to reproduce the downsizing trend of the evolution of the AGN space density, in contrast to recent some SA models. Therefore, reproducing the downsizing trend does not allow for any conclusion on AGN trigger mechanisms.

In order to determine model parameters related to AGNs, we chose parameters to match the optical luminosity function in our model with the observed one at $z = 2$. The observed luminosity function is not corrected for dust obscuration effect. X-ray observations of AGNs show that a significant fraction of AGNs is obscured and the fraction decreases with X-ray luminosity (e.g., Ueda et al. 2003; Hasinger 2008; Merloni et al. 2014). Therefore, dust obscuration can also strengthen the observed downsizing trend of AGN evolution.

In our model, we assume that AGN activity is triggered by major mergers, because major mergers can drive gaseous inflows as shown in some hydrodynamic simulations as described in Section 2.2. Recent observations show that the majority of host galaxies of faint AGNs are disk-dominated galaxies (Georgakakis et al. 2009; Schawinski et al. 2011), while bright AGNs appear to be driven by major mergers (Treister et al. 2012). Therefore, this suggests that it is necessary to include other AGN trigger mechanisms to explain the evolution of AGNs. However, since the cold gas decreases with cosmic time, it is expected that the space densities of bright AGNs decrease more quickly than those of faint AGNs even if we adopt other AGN trigger mechanisms.

At low redshifts ($z \lesssim 1$), the faint AGN space density in our model is larger than the observed faint AGN density (see Figure 2). This suggests that the cold gas mass accreted on a SMBH in our model is too large at $z \lesssim 1$. In our model, we assume that during a major merger, all cold gas supplied from a host galaxy accretes onto a SMBH. However, all the gas that is driven into the central region of the galaxy is not accreted onto the SMBH. Since the angular momentum of cold gas cannot be thoroughly removed, the cold gas forms a circumnuclear disk in the central $\sim$ 100 pc around the SMBH. Kawakatu & Wada (2008) proposed an evolutionary model of a SMBH and a circumnuclear disk. They found that not all the cold gas supplied from the host galaxy accretes onto the SMBH. This is because part of the gas is used to form stars in the circumnuclear disk. As a result, the final SMBH mass ($M_{\rm SMBH,final}$) is not proportional to the total cold gas mass supplied from host galaxy ($M_{\rm sup}$) during the hierarchical formation of galaxies; $M_{\rm SMBH,final}/M_{\rm sup}$ decreases with $M_{\rm sup}$ increasing. We plan to update our SA model to include this model.

At high redshifts ($z \gtrsim 3$), there is a discrepancy between observational results of faint AGNs space densities. The results of GOODS (Fontanot et al. 2007) and COSMOS (Ikeda et al. 2011, 2012; Masters et al. 2012) showed that the faint AGN space density decreases with redshift (see Figure 2). Our model result is consistent with these observational results. The results of Glikman et al. (2010, 2011), however, showed constant or higher space densities of AGNs with $M_{1450} \gtrsim -24$. Since not all of the observations take dust obscuration correction into account, the results do not depend on the recipe of dust correction. Both of Ikeda et al. (2011) and Masters et al. (2012) provide a comment on the discrepancy that the larger space density obtained by Glikman et al. (2010, 2011) can be attributed to a large fraction of contaminants such as Lyman-Alpha Emitters and Lyman-Break Galaxies. Further observations of faint AGNs in a wider survey area are crucial to obtain AGN space densities. A forthcoming wide-field survey using the *Subaru* Telescope with Hyper Suprime-

Cam (Miyazaki et al. 2006, 2012)[6] will provide useful constraints on the SMBH and AGN evolution model.

We appreciate the detailed reading and useful suggestions of anonymous referee that have improved our paper. We thank H. Ikeda for providing us with the compiled observational data of the quasar space density. We also thank N. Kawakatu, K. Wada, T. Nagao, T. R. Saitoh, and S. Ichikawa for useful comments and discussion. Numerical computations were partially carried out on Cray XT4 at Center for Computational Astrophysics, CfCA, of National Astronomical Observatory of Japan. T.I. is financially supported by MEXT HPCI STRATEGIC PROGRAM and MEXT/JSPS KAKENHI grant No. 24740115. M.N. is supported by the Grant-in-Aid (Nos. 22740123 and 25287049) from the Ministry of Education, Culture, Sports, Science, and Technology (MEXT) of Japan.

APPENDIX

GAS, STAR AND SMBH EVOLUTION IN A STARBURST GALAXY

In this appendix, we summarize our model of gas, star and SMBH evolution during a starburst event. We use a simple instantaneous recycling approximation model of star formation, supernovae feedback, and chemical enrichment. The following differential equations describe the evolution of the mass of cold gas $M_{\rm cold}$, hot gas $M_{\rm hot}$, long lived stars $M_{\rm star}$ and SMBH $M_{\rm BH}$ at each time step:

$$\dot{M}_{\rm cold} = -\alpha\psi(t) - \beta\psi(t) - f_{\rm BH}\psi(t), \tag{A1}$$

$$\dot{M}_{\rm hot} = \beta\psi(t), \tag{A2}$$

$$\dot{M}_{\rm star} = \alpha\psi(t), \tag{A3}$$

$$\dot{M}_{\rm BH} = f_{\rm BH}\psi(t), \tag{A4}$$

where $\psi(t) = M_{\rm cold}/\tau_*$ is star formation rate, α is a locked-up mass fraction, and β is the efficiency of reheating for starburst. In this paper, we set $\alpha = 0.75$ in order to be consistent with a stellar evolution model. β is the starburst supernovae feedback strength, which is given by $\beta = (V_{\rm b}/V_{\rm hot})^{-\alpha_{\rm hot}}$, where $V_{\rm b}$ is the velocity dispersion of the newly formed bulge. The solutions of these equations are as follows.

$$M_{\rm cold} = M^0_{\rm cold} \exp\left[-\left(\alpha+\beta+f_{\rm BH}\right)\frac{t}{\tau_*}\right], \tag{A5}$$

$$M_{\rm hot} = M^0_{\rm hot} + \beta\Delta M_*, \tag{A6}$$

$$M_{\rm star} = M^0_{\rm star} + \alpha\Delta M_*, \tag{A7}$$

$$M_{\rm BH} = M^0_{\rm BH} + f_{\rm BH}\Delta M_*, \tag{A8}$$

where t is the time since the starburst, $M^0_{\rm cold}, M^0_{\rm hot}$, $M^0_{\rm star}$ and $M^0_{\rm BH}$ are the masses of cold gas, hot gas, stars and SMBH in progenitor galaxies at the initial state $t = 0$, and $\Delta M_* = (M^0_{\rm cold} - M_{\rm cold})/(\alpha+\beta+f_{\rm BH})$ is the mass of total formed stars.

When a starburst occurs, stars are formed on a very short timescale. Thus, the starburst corresponds to $t/\tau_* \to \infty$ in the above solutions. Therefore, the changes of masses are given by

$$M_{\rm cold} = 0, \tag{A9}$$

$$M_{\rm hot} = M^0_{\rm hot} + \frac{\beta M^0_{\rm cold}}{\alpha+\beta+f_{\rm BH}}, \tag{A10}$$

$$M_{\rm star} = M^0_{\rm star} + \frac{\alpha M^0_{\rm cold}}{\alpha+\beta+f_{\rm BH}}, \tag{A11}$$

and the total star mass formed at starburst becomes

$$\Delta M_{*,\rm burst} = \frac{M^0_{\rm cold}}{\alpha+\beta+f_{\rm BH}}. \tag{A12}$$

From Equation (A12), we can obtain the mass of cold gas accreted onto a black hole [Equation (4)].

REFERENCES

Barnes, J. E., & Hernquist, L. 1996, ApJ, 471, 115
Binney, J.& Tremaine, S. 1987, Galactic Dynamics (Princeton, NJ: Princeton Univ. Press)
Bonoli, S., Marulli, F., Springel, V., et al. 2009, MNRAS, 396, 423
Bower, R. G., Benson, A. J., & Crain, R. A. 2012, MNRAS, 422, 2816
Bower, R. G., Benson, A. J., Malbon, R., et al. 2006, MNRAS, 370, 645
Cattaneo, A., Blaizot, J., Devriendt, J. & Guiderdoni, B. 2005, MNRAS, 364, 407
Cattaneo, A., Dekel, A., Faber, S. M., & Guiderdoni, B. 2008, MNRAS, 389, 567
Cirasuolo, M., McLure, R. J., Dunlop, J. S., et al. 2010, MNRAS, 401, 1166

[6] http://www.naoj.org/Projects/HSC/index.html

Croom, S. M., Richards, G. T., Shanks, T., et al. 2009, MNRAS, 399, 1755
Croton, D. J., Springel, V., White, S. D. M., et al. 2006, MNRAS, 365, 11
Davis, M., Efstathiou, G., Frenk, C. S. & White, S. D. M. 1985, ApJ, 292, 371
Degraf, C., Di Matteo, T., & Springel, V. 2010, MNRAS, 402, 1927
Dekel, A., & Birnboim, Y. 2006, MNRAS, 368, 2
Di Matteo, T., Springel, V. & Hernquist, L. 2005, Nature, 7026, 604
Enoki, M., Inoue, K. T., Nagashima, M. & Sugiyama, N. 2004, ApJ, 615, 19
Enoki, M., Nagashima, M. & Gouda, N. 2003, PASJ, 55, 133
Fanidakis, N., Baugh, C. M., Benson, A. J., et al. 2012, MNRAS, 419, 2797
Ferrarese, L. & Merritt, D. 2000, ApJ, 539, L9
Fontanot, F., Cristiani, S., Monaco, P., et al. 2007, A&A, 461, 39
Fontanot, F., De Lucia, G., Monaco, P., Somerville, R. S., & Santini, P. 2009, MNRAS, 397, 1776
Fontanot, F., Monaco, P., Cristiani, S.,& Tozzi, P. 2006, MNRAS, 373, 1173
Gebhardt, K., Bender, R., Bower, G., et al. 2000, ApJ, 539, L13
Georgakakis, A., Coil, A. L., Laird, E. S., et al. 2009, MNRAS, 397, 623
Glikman, E., Bogosavljević, M., Djorgovski, S. G., et al. 2010, ApJ, 710, 1498
Glikman, E., Djorgovski, S. G., Stern, D., et al. 2011, ApJ, 728, L26
Graham, A. W., 2012, ApJ, 746, 113
Gültekin, K., Richstone, D. O., Gebhardt, K., et al. 2009, ApJ, 698, 198
Guo, Q., White, S., Angulo, R. E., et al. 2013, MNRAS, 428, 1351
Häring, N. & Rix, H. 2004, ApJ, 604, L89
Hasinger, G. 2008, A&A, 490, 905
Hasinger, G., Miyaji, T. & Schmidt, M., 2005, A&A, 441, 417
Henriques, B. M. B., White, S. D. M., Thomas, P. A., et al. 2013, MNRAS, 431, 3373
Hirschmann, M., Dolag, K., Saro, A., Borgani, S., & Burkert, A. 2014, MNRAS, 442, 2304
Hirschmann, M., Somerville, R. S., Naab, T. & Burkert, A. 2012, MNRAS, 426, 237
Hopkins, P. F., Hernquist, L., Cox, T. J., et al. 2005, ApJ, 630, 705
Hopkins, P. F., Hernquist, L., Cox, T. J., et al. 2006, ApJS, 163, 1
Ikeda, H., Nagao, T., Matsuoka, K., et al. 2011, ApJ, 728, L25
Ikeda, H., Nagao, T., Matsuoka, K., et al. 2012, ApJ,756, 160
Ishiyama, T., Fukushige, T. & Makino, J., 2009, PASJ, 61, 1319
Ishiyama, T., Nitadori, K. & Makino, J., 2012, in Proc. Int. Conf. High Performance Computing, Networking, Storage and Analysis, SC f12 (Los Alamitos, CA: IEEE Computer Society Press), 5:1.5:10 (arXiv:1211.4406)
Kauffmann, G., & Haehnelt, M. G., 2000, MNRAS, 311, 576
Kauffmann, G., & Haehnelt, M. G., 2002, MNRAS, 332, 529
Kawakatu, N. & Wada, K., 2008, ApJ, 681, 73
Khandai, N., Di Matteo, T., Croft, R., et al. 2014, arXiv:1402.0888
Komatsu, E., Smith, K. M., Dunkley, J., et al. 2011, ApJS, 192, 18
Kormendy, J. & Ho, L. C., 2013, ARA&A, 51, 511
Magorrian, J., Tremaine, S., Richstone, D., et al. 1998, AJ, 115, 2285
Makino J., & Hut P., 1997, ApJ, 481, 83
Marconi, A., & Hunt, L. K. 2003, ApJ, 589, L21
Marulli, F., Bonoli, S., Branchini, E., Moscardini, L. & Springel, V. 2008, MNRAS, 385, 1846
Masters, D., Capak, P., Salvato, M., et al. 2012, ApJ, 755, 169
McConnell, N. J. & Ma, C.-P., 2013, ApJ, 764, 181
Menci, N., Fiore, F., & Lamastra, A. 2013, ApJ, 766, 110
Merloni, A., Bongiorno, A., Brusa, M., et al. 2014, MNRAS, 437, 3550
Mihos, J. C., & Hernquist, L. 1994, ApJ, 431, L9
Mihos, J. C., & Hernquist, L. 1996, ApJ, 464, 641
Miyazaki, S., Komiyama, Y., Nakaya, H., et al. 2006, Proc. SPIE, 6269, 62690B
Miyazaki, S., Komiyama, Y., Nakaya, H., et al. 2012, Proc. SPIE, 8446, 84460Z
Monaco, P., Fontanot, F. & Taffoni, G. 2007 MNRAS, 375, 1189
Nagashima, M. & Yoshii, Y. 2004, ApJ, 610, 23
Nagashima, M., Yahagi, H., Enoki, M., Yoshii, Y. & Gouda, N. 2005, ApJ, 634, 26
Nobuta, K., Akiyama, M., Ueda, Y., et al. 2012, ApJ, 761, 143
Salucci, P., Szuszkiewicz, E., Monaco, P., & Danese, L. 1999, MNRAS, 307, 637
Schawinski, K., Treister, E., Urry, C. M., et al. 2011, ApJ, 727, L31
Shankar, F., Salucci, P., Granato, G. L., De Zotti, G. & Danese, L. 2004, MNRAS, 354, 1020
Shen, Y. & Kelly, B. C. 2012, ApJ, 746, 169
Somerville, R. S., Hopkins, P. F., Cox, T. J., Robertson, B. E. & Hernquist, L. 2008, MNRAS, 391, 481
Treister, E., Schawinski, K., Urry, C. M., & Simmons, B. D. 2012, ApJ, 758, L39
Ueda, Y., Akiyama, M., Ohta, K. & Miyaji, T. 2003, ApJ, 598, 886
Weinmann, S. M., Pasquali, A., Oppenheimer, B. D., et al. 2012, MNRAS, 426, 2797

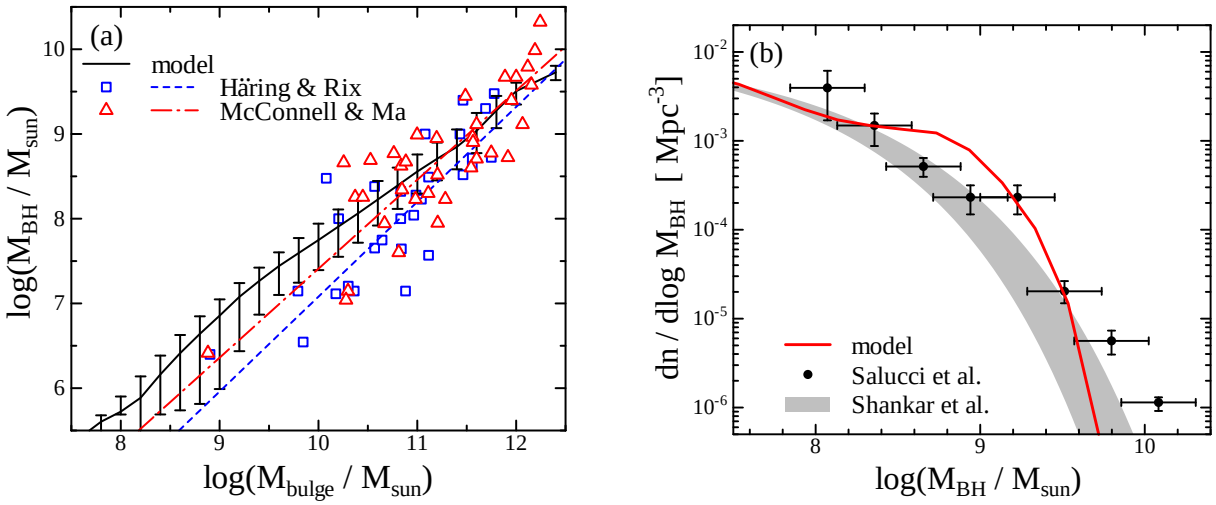

FIG. 1.— Comparison of our SA model results to observations for SMBHs of the presentday universe. (a) Bulge – SMBH mass relation. The solid line indicates the median model results. The ranges represented by vertical solid lines indicate the $10-90$th percentiles. Observational data are represented by squares (Häring & Rix 2004) and triangles (McConnell & Ma 2013). Best-fit power-law relations to the observational data are also provided as dashed (Häring & Rix 2004) and dot-dashed (McConnell & Ma 2013) lines. (b) Black hole mass function. The solid line is the model. Observational data are represented by the symbols (Salucci et al. 1999) and the shaded area (Shankar et al. 2004).

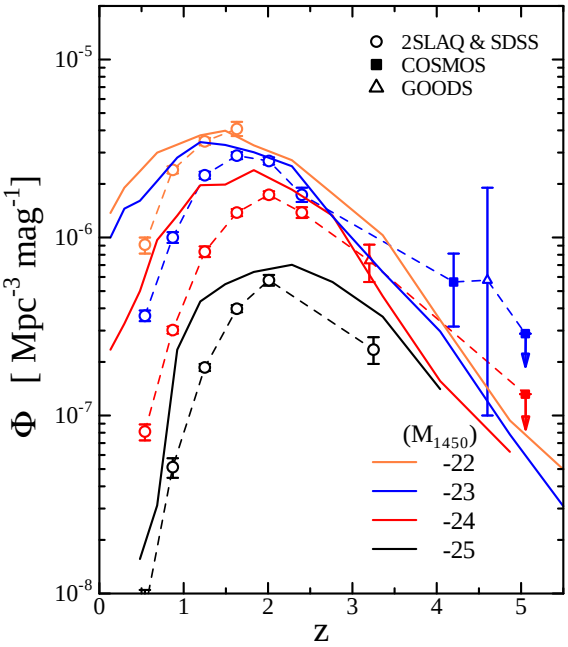

FIG. 2.— Redshift evolution of the AGN space density. Orange, blue, red, and black lines are space density of AGN with $M_{1450} = -22, -23, -24$, and -25, respectively. Solid lines show model results. Symbols with error bars linearly connected with dashed lines are observations: 2SLAQ and SDSS (circles; Croom et al. 2009); GOODS (triangles; Fontanot et al. 2007), and COSMOS (filled squares; Ikeda et al. 2011, 2012).

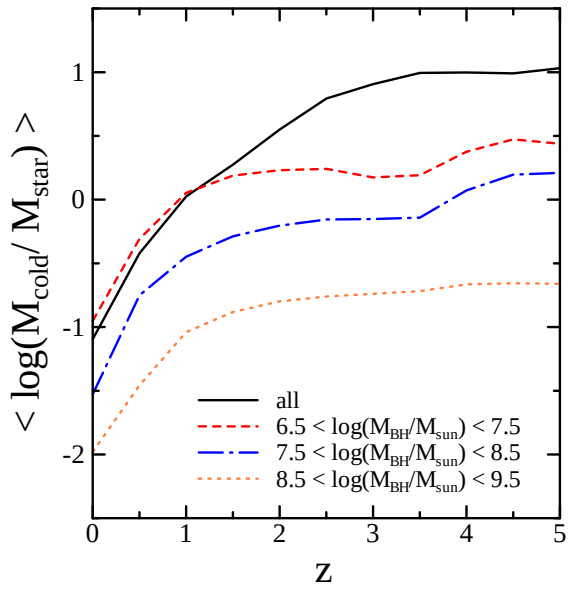

FIG. 3.— Redshift evolution of the ratios of cold gas mass to stellar mass ($\langle \log[M_{\rm cold}/M_{\rm star}] \rangle$) for galaxies with $M_B < -18$. The solid line indicates the logarithmic mean for all galaxies with $M_B < -18$. The dashed, dot-dashed, and dotted lines indicate the mean in different SMBH mass intervals $6.5 < \log(M_{\rm BH}/M_\odot) < 7.5$, $7.5 < \log(M_{\rm BH}/M_\odot) < 8.5$ and $8.5 < \log(M_{\rm BH}/M_\odot) < 9.5$, respectively.

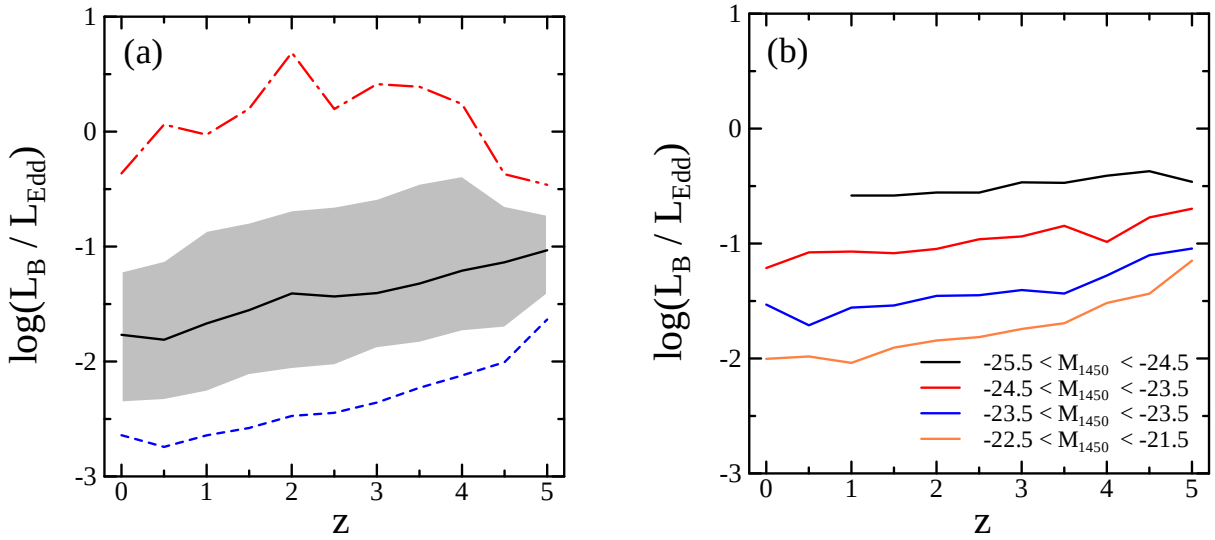

FIG. 4.— Redshift evolution of the B-band Eddington ratios ($\log[L_B/L_{\rm Edd}]$) for AGNs with $M_{1450} < -21.5$. (a) The solid line indicates the median. The shaded area indicates $10-90$th percentiles. The dot-dashed line shows the maximum value and the dashed line shows the minimum value. (b) The solid lines indicate the mean in different magnitude intervals $-22.5 < M_{1450} < -21.5$ (orange line), $-23.5 < M_{1450} < -22.5$ (blue line), $-24.5 < M_{1450} < -23.5$ (red line), and $-25.5 < M_{1450} < -24.5$ (black line).

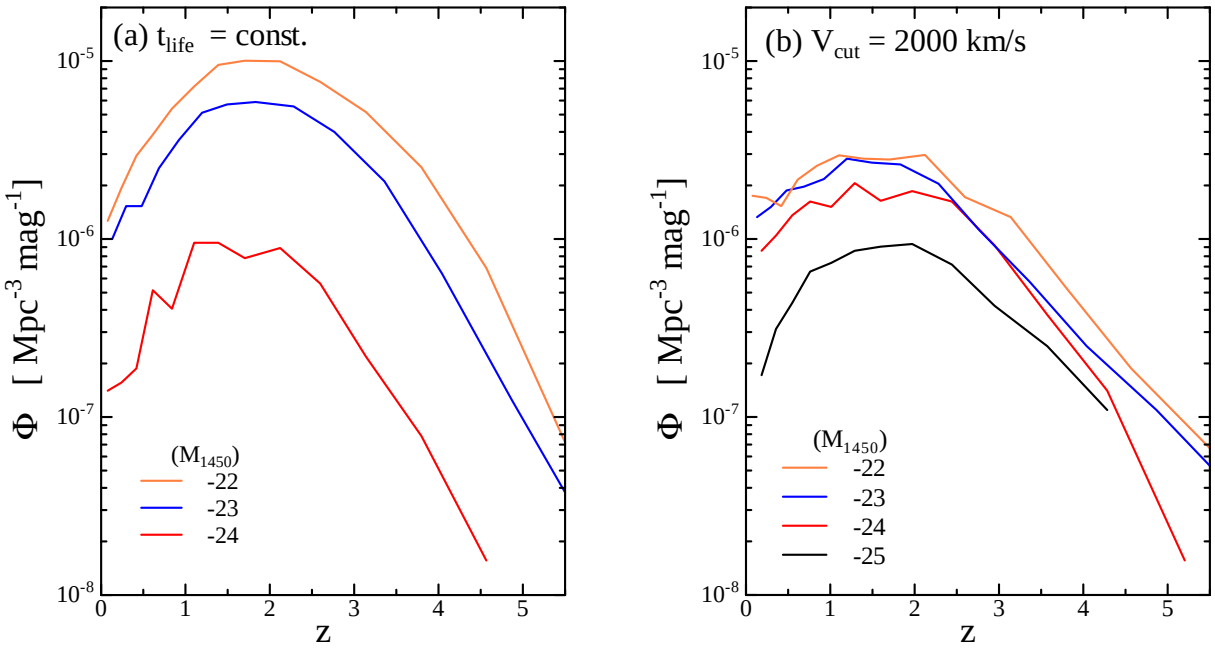

FIG. 5.— Redshift evolution of the AGN space density of results for (a) the constant AGN lifetime model for $t_{\rm life} = 5.0 \times 10^7$ yr and (b) $V_{\rm cut} = 2000$ km s^{-1}. Orange, blue, red, and black lines are space density of AGNs with $M_{1450} = -22, -23, -24$, and -25, respectively.